

AD-A101 170 CALIFORNIA UNIV SAN DIEGO LA JOLLA INST FOR PURE AND--ETC F/6 20/5
LONG PULSE XECL LASER FREQUENCY DOWN CONVERSION AND LOW VOLTAGE--ETC(U)
MAY 81 J I LEVATTER, S C LIN N00014-79-C-0955
NL

UNCLASSIFIED

1 OF 1
404
101 70

END
DATE
FILED
7-81
DTIC

DTIC FILE COPY

AD A101170

11 Long Pulse XeCl Laser Frequency Down Conversion
and

Low Voltage, Low Energy X-Ray Preionization Source

10 J. I. Levatter and S. C. Lin

Institute for Pure and Applied Physical Sciences
University of California, San Diego, La Jolla, CA 92093

9 Final Report Oct 79 - Mar 81

11 May 81

Contract No. N00014-79-C-0955

15 395-599-REB

12 26

Prepared for
The Office of Naval Research
Arlington, VA 22217

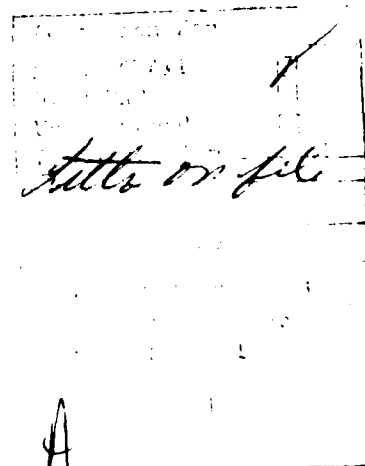
This document has been approved
for public release and sale; its
distribution is unlimited.

403608 14

816 01087

Table of Contents

	Page
I. Introduction	4
II. Long Pulse XeCl Laser Frequency Down Conversion	5
References	7
III. Low Voltage, Low Energy X-ray Preionization Source	12
References	19



A

List of Figures

<u>Section II</u>		<u>Page</u>
Fig. 1	Block diagram and electrical network of UCSD large volume x-ray preionization laser	8
Fig. 2	Near and far-field burn pattern from 1 liter volume XeCl laser	9
Fig. 3	Experimental arrangement of Pb vapor Raman down conversion	10
Fig. 4	Typical frequency down conversion results showing the input UV (a), the blue-green output (b), and the depleted pump signal (c). These data were taken with the Pb cell at $\sim 1150^{\circ}\text{C}$ using 20 Torr of argon as a buffer gas	11
<u>Section III</u>		
Fig. 1	Electrical schematic of x-ray pulser. Thyratron filament transformers are not shown for clarity	24
Fig. 2	Physical layout of x-ray source showing the e-beam and HV pulser assembly	25
Fig. 3	Electron beam voltage (a) and current density (b) produced by the electron-gun diode. Both traces were taken at a 35 Hz repetition rate and represent at least 20 overlaid traces	26

I. Introduction

This report covers the results of two small research programs (Contract #N00014-79-C-0955) carried out at UCSD between October 1979 and March 1981. The first program, "Long Pulse XeCl Laser Frequency Down Conversion," was initiated following the encouraging Raman shifting results, obtained by Ralph Burnham at NRL. The second program, "Low Voltage, Low Energy X-Ray Preionization Source" was undertaken after it was realized that the energy and power scaling of certain avalanche discharge excited lasers required a reliable, non-contaminating volumetric source of electron preionization as could be provided by moderate energy x-rays.

The Raman down shifting project was a continuation of the joint one week long experiment conducted at UCSD by Ralph Burnham (NRL) and Jeff Levatter (UCSD). In this initial experiment, the 308 nm UV output from the UCSD XeCl laser (see Fig. 1) was focused into a lead vapor (Pb) heat pipe and the stimulated Raman emission in the blue-green was monitored. The research which followed this preliminary experiment involved the refinement of the Raman down conversion experiment which consisted primarily of the improvement of the XeCl laser mode quality. This work and the results thereof are discussed in Section II, of this report.

Section III of this report describes the results of an engineering program to build a reliable low energy X-ray source suitable for the

preionization of rare-gas/halide and mercury-halide discharge excited lasers. The information in this section is contained in the form of a paper which has been submitted to the Review of Scientific Instruments. The paper describes the construction, operation, and performance of the new x-ray device.

II. Long Pulse XeCl Laser Frequency Down Conversion

The initial Pb vapor downshifting experiment conducted in conjunction with Dr. Burnham used the UCSD XeCl laser fitted with a "lens" ³ unstable resonator. In this optical configuration the laser produced a relatively poor beam quality in which more than two-thirds of the laser output energy was emitted in the form of unusable highly divergent parasitic modes. This resulted in a relatively poor Raman conversion efficiency of only a few percent, and in damaging many of the Suprasil I quartz lenses used in the optical arrangement. The damage was caused by hot spots in the laser beam intensity profile caused by high order parasitics, not by a lack of laser gain uniformity. ²

Following these initial experiments the laser mode quality was improved by changing the optical resonator and by sandblasting the XeCl laser discharge electrodes to reduce transverse optical reflections. The new resonator employed a concave 10 m total reflector and a convex 6.68 m partial reflector ($R \approx 17\%$) to form a positive branch unstable resonator. The magnification of the resonator was rather low ($M = 1.4$); nevertheless, this optical arrangement produced a very uniform near-field laser intensity distribution ($3 \times 3 \text{ cm}^2$) and a moderately good

far-field pattern, as can be seen in the burn pattern shown in Fig. 2.

The laser energy passed through a 10 \times diffraction limited hole was $\sim 1/2$ the near field energy.

The experimental arrangement used for the Raman conversion experiment is detailed in Fig. 3. The output of the XeCl laser was focused by a 2 meter quartz lens into a 65 cm long Pb vapor cell. The light exiting the Pb cell was split and appropriately filtered in order to monitor the input UV, the generated blue-green, and the depleted UV. Typical results are shown in Fig. 4.

The overall energy conversion efficiency was not as good as expected. Only $\sim 20\%$ of the input energy was shifted to the blue-green. However, near the peak of the 459 nm output pulse, the power conversion efficiency was nearly 50%. The lower overall efficiency was due to the fact that the blue-green output was only ~ 40 nsec (FWHM) long while the input pump pulse was ~ 100 nsec in duration. One likely explanation for the shortened Raman shifted pulse is the dynamics of the XeCl laser mode structure. According to Goldhar et al., ⁴ the time evolution of a developing low-order mode in an unstable resonator goes as $1/M$, where M is the resonator magnification. Therefore, only during the latter part of the UV input pulse was the UV beam near diffraction limited. And only when the laser output is near diffraction limited can it be focused tightly enough to produce a sufficient power density in the Pb vapor to obtain efficient non-linear conversion. Another possibility which could explain

the poor conversion, was an insufficient lead density in the heat pipe, although calculations indicate this should not have been a problem. After it was realized that the resonator magnification was insufficient, the experiment was terminated.

Although a high Raman conversion efficiency was not achieved in this limited set of experiments several important results were obtained that impact the Pb vapor downshifting technique as a means of generating high average power blue-green laser output. First, efficient non-linear frequency conversion requires a homogeneous laser gain to avoid parasitic modes and hot spots which can easily damage optical components. Second, the laser oscillator should be designed so that the mode structure is in steady state. This can be accomplished by using a high magnification unstable resonator ($M \geq 5$), a MOPA system, or an injection locked oscillator configuration. And third, a high energy, high efficiency ($3 \sim 50\%$) conversion seems possible provided the UV laser beam quality is sufficient to allow the propagation of a collimated pump beam through the Pb vapor in order to create a high power density pump beam and at the same time have an adequate number of Pb atoms in the pump volume. Since all of the above points can be achieved in a properly designed system, an efficient, high energy blue-green laser should be possible.

References for Section I

1. R. Burnham and N. Djeu, Opt. Soc. Amer. 3, 215 (1978).
2. S. C. Lin and J. I. Levatter, Appl. Phys. Lett. 34, 505 (1979).
3. D. L. Barker and T. R. Loree, Appl. Opt. 16, 1792 (1977).
4. J. Goldhar, W. R. Rapoport, and J. Murray, IEEE J. Q.E., 16, 235 (1980).

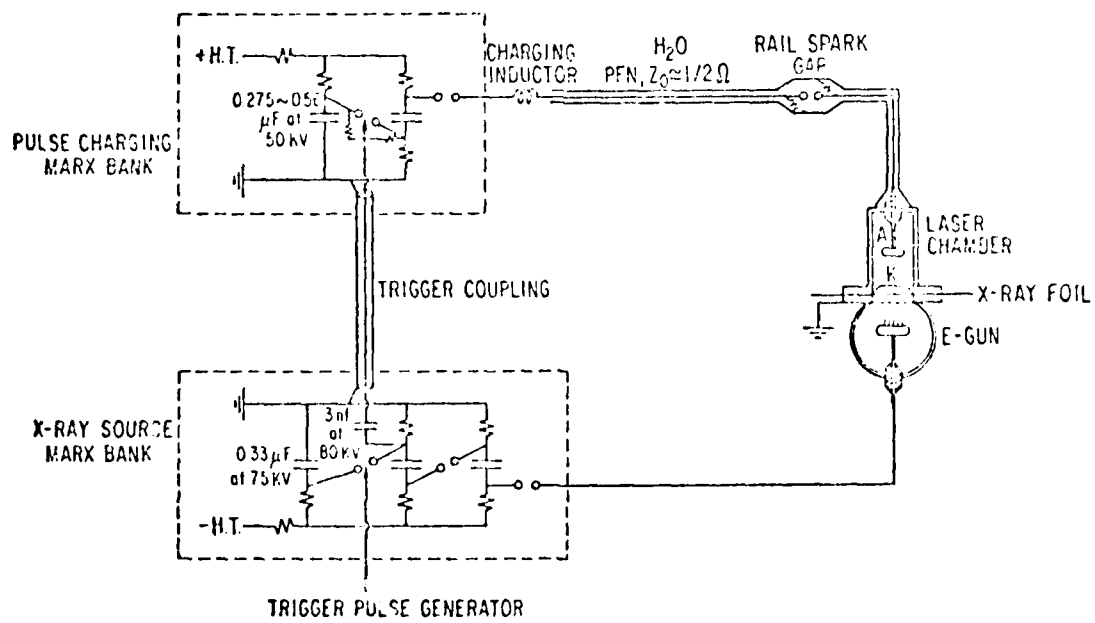
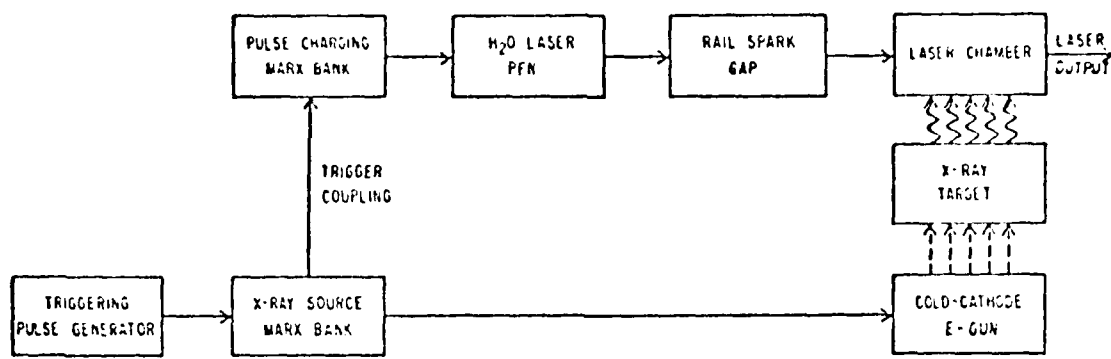
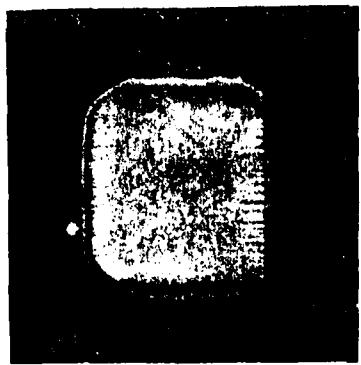


Fig. 1. Block diagram and electrical network of UCSD large volume x-ray preionization laser.

XeCl BEAM QUALITY (1 LITER DISCHARGE)

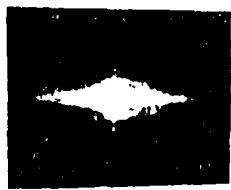
UNSTABLE RESONATOR USED ($M \approx 1.4$)

NEAR FIELD



ENERGY $\approx 1.5-2.5$ J

FOCUS OF
2 METER
LENS



USABLE ENERGY
0.86 TO 1.5 J

FIG. 2. Beam quality for various parameters: 1 liter XeCl laser.

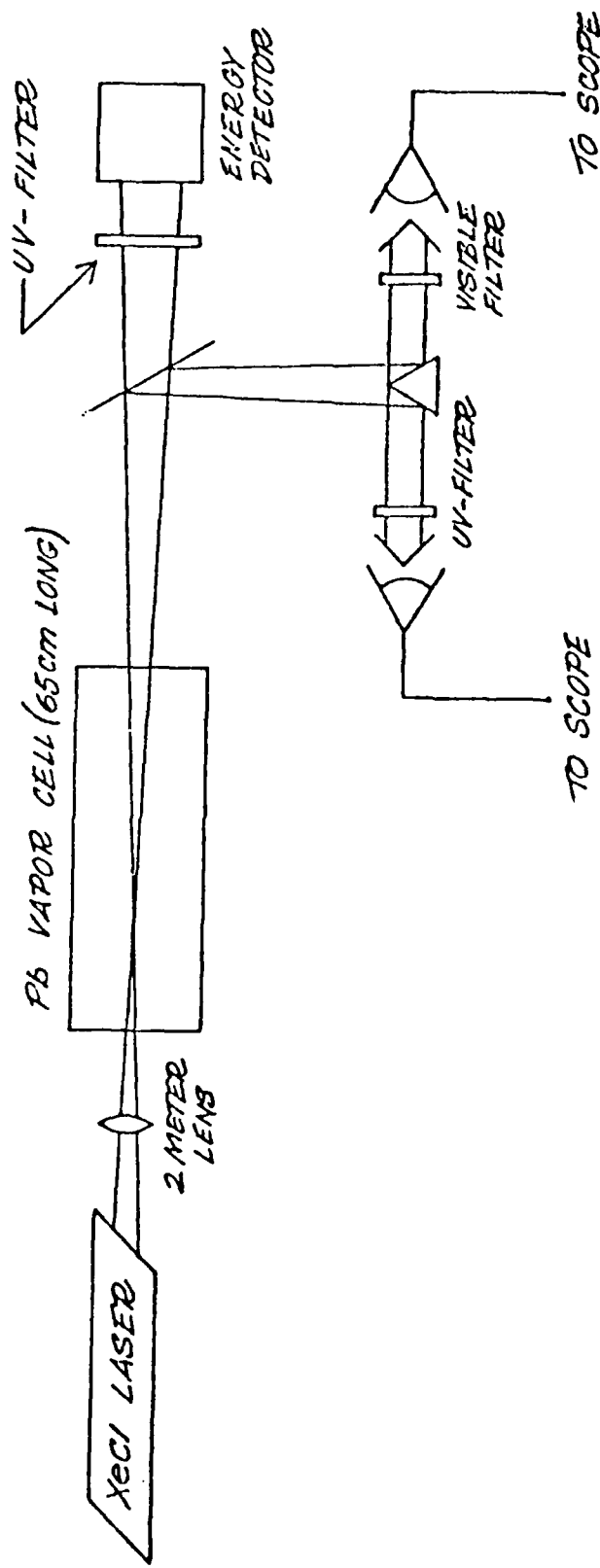
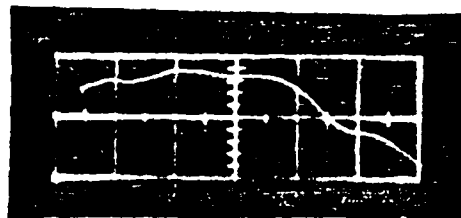


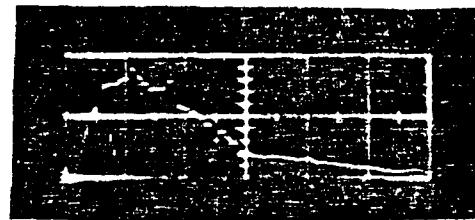
Fig. 3. Experimental arrangement of Pb vapor Raman down conversion.

INPUT-UV
 $E=0.86\text{ J}$
 20 nsec/cm



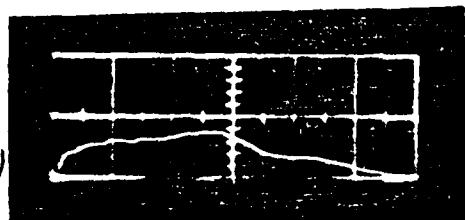
(a)

OUTPUT-459 nm
 $E=0.132\text{ J}$
 20 nsec/cm



(b)

DEPLETED UV
 20 nsec/cm
(~40% REMAINING)



(c)

Fig. 4. Typical frequency down conversion results showing the input UV (a), the blue-green output (b), and the depleted pump signal (c). These data were taken with the Pb cell at $\sim 1150^\circ\text{C}$ using 20 Torr of argon as a buffer gas.

II. (Contract Title): Low Voltage, Low Energy X-Ray
Preionization Source

Low Energy X-Ray Preionization Source for Discharge
Excited Lasers

Abstract

A low voltage (50 kV) low energy (3 J) x-ray preionization source has been developed specifically for avalanche discharge laser preionization. The new device uses a single stage high voltage capacitor switched by a gradient grid hydrogen thyratron that drives a cold-cathode electron beam. Intense x-ray emission is produced by allowing the e-beam to impact a high Z target foil. The entire system can operate up to 35 Hz repetition rate and produce an electron preionization density of $\sim 10^8 \text{ cm}^{-3}$ in most rare-gas/halide laser gas mixtures.

I. INTRODUCTION

The intrinsically large mass-penetration-power¹ of moderate energy x-rays ($10 \text{ keV} < E < 200 \text{ keV}$) makes them an ideal source of preionization for avalanche discharge excited lasers.^{2,3} Calculations⁴ and previous experiments³ indicate that a total pulse energy of only $\sim 1 \text{ J}$ is sufficient to create enough x-rays to preionize a discharge volume on the order of 1 m^3 . At this small energy, a pulsed x-ray source becomes a very attractive means of preionizing many different high energy and high repetition rate gas discharge lasers.

With this application in mind, a new pulsed x-ray source system has been developed at UCSD. It operates at relatively low voltage ($\sim 50 \text{ kV}$) and energy ($\sim 3 \text{ J/pulse}$), and it is capable of producing volumetric preionization densities of $\sim 10^8 \text{ cm}^{-3}$ in CO_2 and most rare-gas/halide (RGH) laser systems. In this device x-rays are generated by an electron-beam impinging on a thin tantalum target foil, producing a spatially isotropic beam of x-rays in the forward and backward directions, with the forward scattered x-rays being used for convenience. The e-beam consists of a hydrogen thyratron switched cold-cathode e-gun that produces a current density of $2-3 \text{ A/cm}^2$ at a beam voltage of $50-60 \text{ kV}$ over an area of $1.5 \times 60 \text{ cm}^2$. The duration of the e-beam, and hence, the x-ray pulse, has been kept short ($\sim 150 \text{ nsec}$) to minimize the total pulse energy. The x-ray source operates at a maximum repetition rate of 35 Hz , and is limited only by the 250 watt power supply used.

In the sections which follow, the operating principles and the important construction details of the new x-ray source will be described. Measurements of the e-beam current density and generated x-ray flux will also be outlined, and lastly, specific applications to RGH lasers will be explored.

II. PULSED X-RAY GENERATOR

The x-ray source contains three primary subsystems: (a) the high voltage (HV) pulser that provides power to the e-beam, (b) the cold-cathode electron beam gun, and (c) the x-ray converter (e-beam target). Each of these subsystems is described in the following sections.

A. HV Pulser

This subsystem is the key to proper operation of the x-ray source. Initially, the electrical and physical layout of the HV pulser, as well as its output characteristics, are discussed. In addition to the consideration of these factors, attention is also given to individual HV component stress, in order to insure a high degree of reliability for the entire x-ray system.

The basic pulse power source consists of a simple single stage HV capacitor switched by an EG&G HY-5301 gradient grid hydrogen thyratron. The electrical schematic of the pulser showing the trigger and bias circuitry is detailed in Fig. 1. The HV capacitor is charged resistively from a dc 50 kV, 5 mA power supply. This voltage level requires that the charging resistor, HV capacitor, and hydrogen thyratron be immersed in oil for

electrical insulation and cooling. The HV capacitor and the thyratron are mounted in a coaxial aluminum housing (Fig. 2) minimizing the total circuit inductance and also reducing thyratron RFI and x-ray emission. The HY-5301 thyratron is the heart of the x-ray source HV pulser. This switch is a pentode consisting of an anode, cathode and three grids. The first or auxiliary grid provides a dc keep-alive current which allows fast tube turn-on and small trigger jitters (~ 2 nsec). The second grid is used for bias and commutation control i.e., trigger control, and the third or gradient grid is biased at one-half the tube charging voltage and doubles the maximum forward voltage hold-off (FHV) of the tube.

When the circuit is initiated by a positive 500 volt signal at the trigger input shown in Fig. 1, the pulser produces a fast rising 50 kV pulse on the e-beam cathode. This voltage is monitored by a capacitive divider on the e-gun feed-through (Fig. 2). As can be seen in Fig. 3(a), the (10-90%) voltage rise time is 60 nsec and its duration is 140 nsec (FWHM). The current passing through the thyratron, on the other hand, is determined by the space-charge controlled impedance of the e-gun diode, and peaks at less than 50 A. This results in a maximum instantaneous switched power of ~ 25 MW, well below the tube rating.

To insure long reliable performance of the pulser, the critical HV components, namely the HV storage capacitor and the hydrogen thyratron switch, have been severely derated in the pulser design. The HV capacitor is rated by the manufacturer at a maximum dc voltage of 80 kV, and the HY-5301 thyratron is rated for 70 kV FHV and 6000 A maximum current. In actual pulser service the

charging voltage never exceeds 60 kV and the pulse current is always less than 500 A, well below the maximum ratings of either component. To date, the pulser has performed quite well without any difficulties up to the maximum repetition rate allowed by the HV power supply, 35 Hz.

B. Cold-Cathode Electron Gun

The electron gun diode is of conventional design. It consists of a 60 cm long cathode inside of an aluminum vacuum chamber fitted with a polycarbonate dielectric HV feedthrough (Fig. 2). The cathode is a 2.54 cm diameter by 65 cm long aluminum rod fitted with either a 0.0005 in. thick tantalum or 0.25 in. thick carbon felt⁵ strip, 60 cm long and 0.5 cm high (in the direction of the electric field). When a high voltage pulse is applied to the cathode structure the sharp field enhanced Ta foil edges or carbon felt fibers produce sufficient field emission to create a moderately dense plasma surrounding the cathode surface.⁶ This transient plasma acts as a virtual cathode (with zero work function) and becomes the e-beam electron source. In operation the Ta foil requires a slightly higher applied voltage than the carbon felt in order to uniformly create the plasma layer along the entire cathode length. The Ta foil cathode operates well at ≥ 50 kV and the carbon felt works well at voltages down to ~ 45 kV. The current density produced by the cold-cathode emitter is controlled, as previously mentioned, by space-charge effects. The space-charge limited current density for a plane-parallel geometry is given by, $j = 2.366 \times 10^{-6} V^{3/2} / d^2 A/cm^2$, where V is the applied voltage and d is the anode-cathode separation. To produce

a current density in the 3 A/cm^2 range, the spacing has been adjusted to $\sim 2 \text{ cm}$.

The only other notable feature regarding the e-gun is the level of vacuum necessary for proper diode operation. At pressures below 10^{-4} Torr the diode performs well, but as the pressure exceeds 10^{-4} Torr the cathode emission becomes non-uniform along the cathode length, and arcing occurs. In order to maintain the pressure in the 10^{-5} to 10^{-4} Torr range, a 2 in. diameter oil diffusion pump fitted with a water-cooled baffle is attached to the vacuum chamber by a 2 in. diameter gate valve. The pumping speed of this system is more than adequate for the 125 W average e-beam power.

C. X-Ray Converter

The x-rays produced in this device are also generated in a fairly conventional manner; namely, a high Z target is bombarded with high energy ($\sim 50 \text{ keV}$) electrons.³ This process produces Bremsstrahlung radiation which is characterized by a continuous photo energy spectrum from zero energy to E_{\max} , with a mean energy at $E_{\max}/2$, where E_{\max} is the energy of the incident electron beam. That is, a 50 keV beam will generate an x-ray spectrum with an E_{\max} of 50 keV and a mean photon energy of $\sim 25 \text{ keV}$. However, when electron energies of $< 100 \text{ keV}$ are involved, only a small fraction of the total e-beam is converted into radiation. The conversion efficiency is roughly $EZ/700$,³ where E is the incident electron energy in units of MeV, and Z is the atomic number of the target material.

To maximize the x-ray conversion efficiency, it is evident that a high Z material such as tungsten, tantalum, or lead is desirable. As such, tantalum ($Z = 73$) in the form of a 0.0003 in. thick foil has been chosen for the low energy x-ray converter because this material has a moderately high Z , and excellent mechanical and thermal properties. A very thin foil is used in order to maximize the forward scattered x-ray intensity. The optimum thickness of this foil is determined by the electron absorption and x-ray transmission characteristics of the target material, and generally turns out to be somewhat less than an electron stopping range (ESR). For 50 keV electrons in Ta the ESR⁷ is 0.009 g/cm^2 or approximately 0.0003 inches.

When the 50 keV e-beam strikes the thin target foil, copious amounts of x-rays are produced, and they exit the e-gun vacuum chamber through a 0.032 in. thick, $60 \times 1.5 \text{ cm}^2$ aluminum x-ray window (transmission $> 90\%$). Since the Td foil is connected to electrical ground and acts as the e-beam anode, at a 35 Hz pulse repetition rate, over 100 W of power is dissipated in the foil. This waste heat is effectively removed by thermal radiation cooling. Because of the high melting temperature of Ta ($> 3000^\circ\text{C}$), this simple cooling method is actually sufficient for pulse repetition rates in the kilohertz range.

III. E-BEAM CURRENT DENSITY AND X-RAY SOURCE STRENGTH

In order to verify the utility of the low energy x-ray source, measurements of the e-beam current density, j , and generated x-ray source strength, S_o , have been made. The outcome of these measurements have been compared with the calculated values of j and S_o , which will also be presented in this section.

The magnitude and time history of the e-beam j was measured by using several discrete Faraday probes placed inside the vacuum chamber. Seven equally spaced $2 \times 1.5 \text{ cm}^2$ copper probes were placed along the 60 cm length of the cathode to sample the longitudinal uniformity and the shot to shot repeatability of the e-beam. The various probe outputs were monitored on a Tektronix 519 oscilloscope. An example of these outputs, at 35 Hz, is shown in Fig. 3(b). The overall beam uniformity was better than $\pm 4\%$ along the 60 cm length, and the shot to shot variation was less than $\pm 2\%$, becoming even better as the repetition rate was increased from a few Hz to 35 Hz.

Although the overall homogeneity of j appears good, it is the uniformity of the x-ray beam that is ultimately important. Since the x-rays were generated by a multiple-scattering process, the spatial distribution of the x-ray source was significantly superior to that of the e-beam; the effect of any non-uniformities in j being largely smeared out. Since it was assumed that the spatial distribution of the x-rays is at least as good as the e-beam j , only the total x-ray flux was measured and compared with the calculated value.

The x-ray source strength was directly inferred from a measurement of the x-ray induced ionization in argon. From Ref. 3 the ionization source strength is related to the electron density by $S_0 = n_e/t$, where t is the duration of the x-ray pulse. The electron density n_e was measured by using an ionization chamber similar to that described in Ref. 3 placed at the x-ray window. The measured value of n_e in argon at 2 atm pressure was $1.2 \times 10^9 \text{ cm}^{-3}$, implying an x-ray source strength of $1 \times 10^{16} \text{ cm}^{-3} \cdot \text{sec}^{-3}$.

Again according to Ref. 3, the generated x-ray source strength is given by

$$S_o = \frac{V j \beta \mu f}{2W} \quad (1)$$

where V and j are the e-beam voltage and current, respectively, β is the x-ray conversion efficiency (see Section II-C), W is the energy needed to produce an electron ion-pair, μ is the x-ray absorption coefficient, and f is a geometric factor including the usable x-ray beam solid angle as well as all other absorption and scattering losses. Using a value of $j = 2 \text{ A/cm}^2$, $V = 50 \text{ kV}$, $\beta = 0.5\%$, $W = 30 \text{ eV} = 3 \times 10^{-18} \text{ J}$ (Ref. 3); $\mu = 2.8 \times 10^{-2} \text{ cm}^{-1}$; and $f = 10^{-2}$, Eq. (1) yields $S_o = 2.2 \times 10^{16} \text{ cm}^{-3} \cdot \text{sec}^{-1}$. This figure is fairly close to the measured value.

IV. APPLICATION TO RGH DISCHARGE EXCITED LASERS

In order to produce a spatially stable high pressure avalanche discharge suitable for RGH laser excitation, a volumetrically uniform preionization density $\geq 10^7 \text{ cm}^{-3}$ must be created in electro-negative gas mixtures.⁴ This can quite easily be accomplished by using the low energy x-ray source described here. The excellent transverse uniformity of the x-ray beam, along with the large mass-penetration power of x-rays, assures the necessary homogeneity of the induced preionization. The magnitude of the ionization density will, however, vary depending on the laser gas composition.

In rare-gas/halide laser gases (unlike argon) the electron density is controlled by electron attachment. In these electro-negative gases the steady-state electron density is related to the ionization source by the simple equation

$$n_e = \frac{S_o}{n_a \beta} \quad (2)$$

where n_a is the number density of the attaching species, and β is the electron attachment coefficient. Because the attachment process is usually very rapid, n_e reaches its steady-state value in only a few nanoseconds at pressures greater than 1 atm.

To calculate the preionization density produced in typical RGH laser gas mixtures, it is also necessary to correct the x-ray source strength in Eqs. (1) and (2) for the appropriate x-ray absorption coefficient, μ . The difference in μ for argon and for the particular gas being preionized can be used to scale the experimentally measured value of S_o ($1.6 \times 10^{16} \text{ cm}^{-3} \text{-sec}^{-1}$). Examples of the x-ray generated preionization for two typical RGH laser gas mixtures are given in the chart below:

Laser Gas	Ar	KrF	XeCl
Mixture	Ar/100	He:Kr:F ₂ /95.9:4:0.1	He:Xe:HC1/95.9:4:0.1
Pressure	2 atm	4 atm	4 atm
$S_o, \text{ cm}^{-3} \text{-sec}^{-1}$	1.2×10^{16}	3.3×10^{15}	5.6×10^{15}
$\mu, \text{ cm}^{-1}$	2.8×10^{-2}	7.8×10^{-3}	1.3×10^{-2}
$\beta, \text{ cm}^{-3} \text{-sec}^{-1}$	--	$\sim 2 \times 10^{-9}$	$\sim 1 \times 10^{-10}$
$n_e, \text{ cm}^{-3}$	1.6×10^9	2×10^7	5×10^8

V. SUMMARY

A low energy, low voltage pulsed x-ray source suitable for the pre-ionization of most RGH laser systems has been constructed. It requires a relatively small electrical input energy (~ 3 J/pulse) and is capable of operating at moderate pulse repetition rates with a small dc power supply. Measurements of the e-beam current density and x-ray source strength show the x-ray generator beam uniformity and intensity adequate to create a volumetric preionization density of $\sim 10^8 \text{ cm}^{-3}$ in most RGH lasers. This level of preionization is more than sufficient to preionize most gas laser discharges homogeneously at pressures up to 20 atm. Thus, the pulsed x-ray preionization generator described in this paper can provide an external, non-contaminating preionization source for discharge excited lasers without the need for fragile foil windows. The present system operates up to 35 Hz with a $1.5 \times 60 \text{ cm}^2$ x-ray beam, but the same general design should be capable of scaling to larger beam areas and kilohertz repetition rates. This type of source may, therefore, help to increase the energy output and average power obtainable from discharge pumped RGH excimer lasers.

REFERENCES

- ¹ G. R. White, X-Ray Attenuation Coefficients from 10 keV to 100 MeV, NBS Report No. 1003 (U. S. GPO, Washington, D.C., 1952).
- ² R. Fujimoto and N. Toshima, Trans. Inst. Eng. Japan 98-C, 133 (1978).
- ³ S. C. Lin and J. I. Levatter, Appl. Phys. Lett. 34, 505 (1979).
- ⁴ J. I. Levatter and S. C. Lin, J. Appl. Phys. 51, 210 (1980).
- ⁵ The carbon felt is a Union Carbide product.
- ⁶ G. Loda, Physics International Final Report #DASA 01-71-C-0111 (1971).
- ⁷ A. T. Nelms, Energy Loss and Range of Electrons and Positrons, NBS Circular 577 (U. S. GPO, Washington, D. C., 1956).

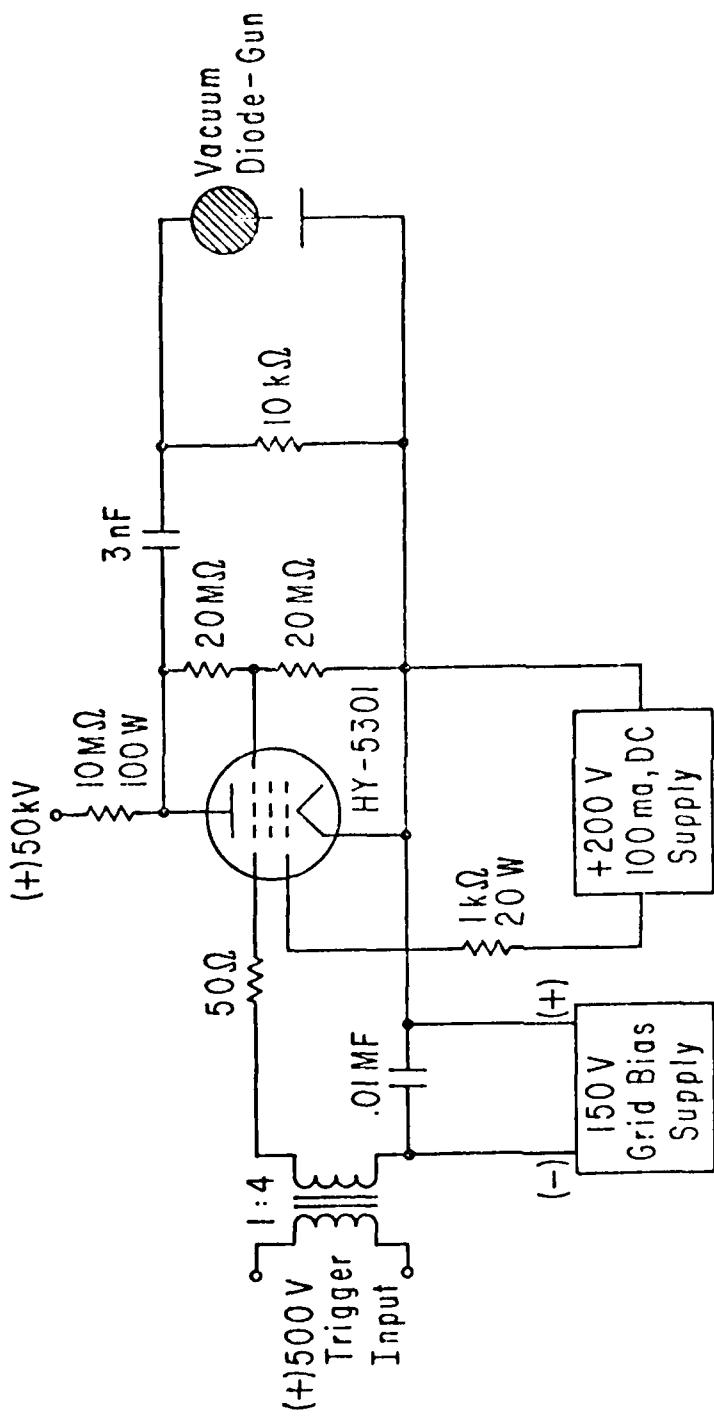


Fig. 1. Electrical schematic of x-ray pulser. Thyatron filament transformers are not shown for clarity.

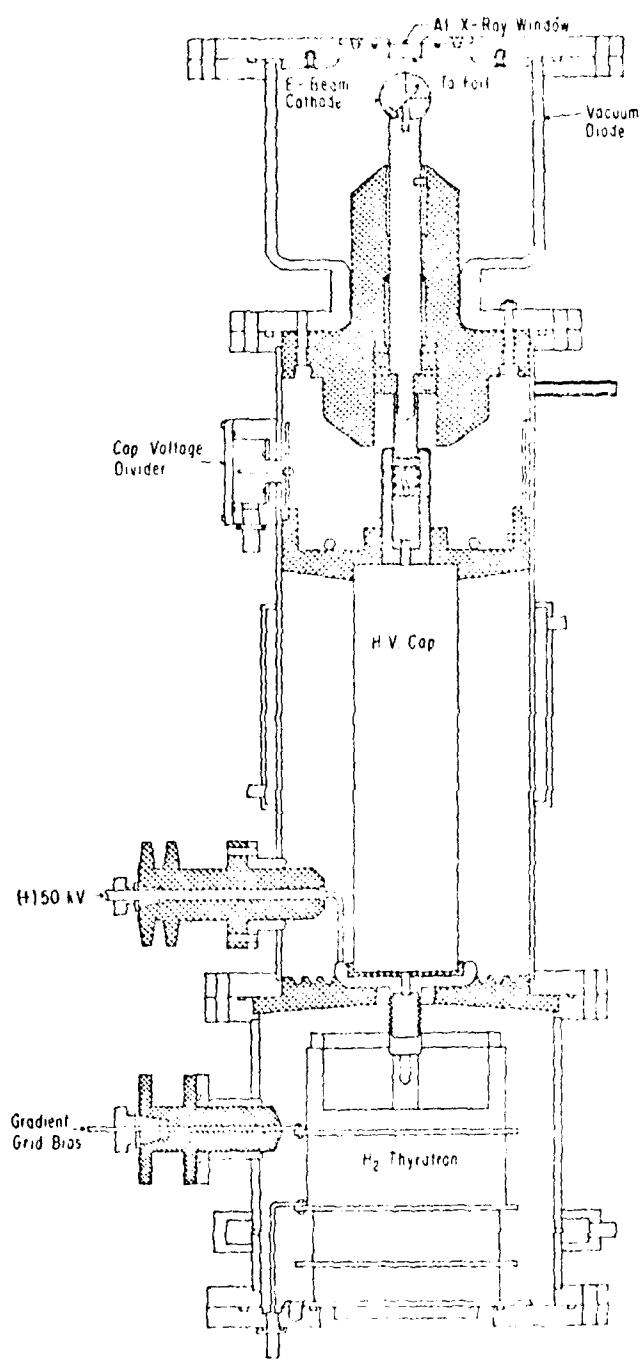


Fig. 2. Physical layout of x-ray source showing the e-beam and HV pulser assembly.

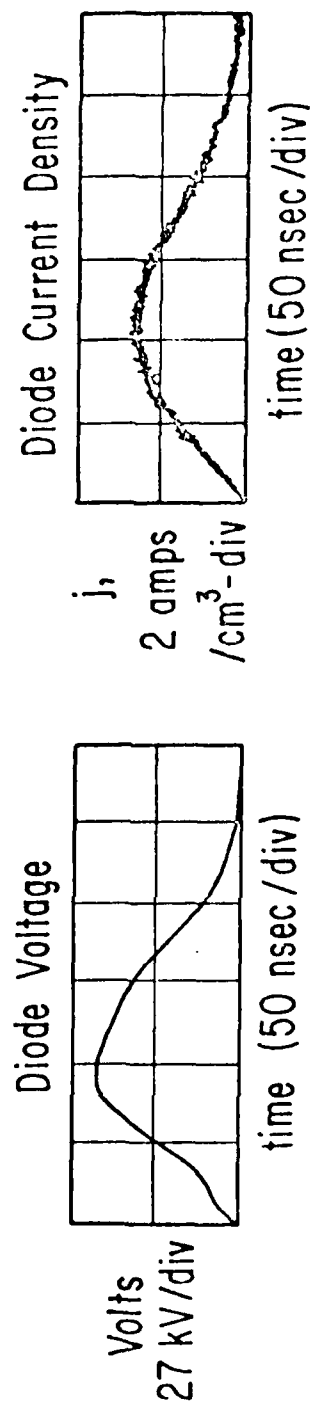


Fig. 3. Electron beam voltage (a) and current density (b) produced by the electron-gun diode. Both traces were taken at a 35 Hz repetition rate and represent at least 20 overlaid traces.

